25th ABCM International Congress of Mechanical Engineering
October 20-25, 2019, Uberlândia, MG, Brazil

COB-2019-1421
EFFECT OF GEOMETRICAL PARAMETERS IN HEAT TRANSFER AND PRESSURE DROP OF SOLAR AIR HEATER WITH RECTANGULAR-WINGLET UNDER LAMINAR FLOW CONDITIONS

Rafael Módolo Dias Duarte
Alexia Ysabelli Antunes
Wallace Gusmão Ferreira
Daniel Jonas Dezan
Federal University of ABC, Av. dos Estados, 5001 – Bangú, Santo André – SP, 09210-580
e-mails: rafael.mdduarte@yahoo.com.br, alexia.ysaantunes@gmail.com, wallace.ferreira@ufabc.edu.br, daniel.dezan@ufabc.edu.br

Abstract. *One of the ways to convert solar energy into thermal energy is by using thermal solar collectors, which absorb the solar radiation in an absorber plate/tube and transfer it to the working fluid. Among the different types of thermal solar collectors, the flat plate solar collector using air as working fluid is widely used. One of the drawbacks of solar air heaters is the low heat convection from the absorber plate to the flowing air; thus, the efficiency of solar air heaters depends greatly in the enhancement of the convective heat transfer coefficient. In this sense, a possible solution to enhance the heat transfer with a minimum pressure loss is to use longitudinal vortex generator (LVG). The present study numerically investigates the influence of three rows of rectangular-winglet (RWL) pairs on the heat transfer enhancement and pressure loss for a laminar flow in a solar air heater, by using the Finite Volume Method (FVM), varying the geometric parameters (chord, height and angle of attack) for each row of RWL.*

Keywords: *longitudinal vortex generators, rectangular-winglet vortex generators, solar air heaters, sensitivity analysis, computational fluid dynamics*

1. INTRODUCTION

It is known that the demand for energetic resources grows every year around the world. Schutz et al. (2013) reported that there would be an estimated growth in the world energy consumption from 573 quadrillion of BTUs, in 2015, to 770 quadrillion of BTUs, in 2035, corresponding to an increase of 34.38 % on the energy consumption. Some of the problems of energy production are based on non-renewable energy sources, such as fossil fuels. Among all the renewable energy source options, one of them, which is viable for Brazil, is the solar energy. As explained by Shahsavari and Akbari (2018), the solar energy is zero air pollutant during power generation, reducing considerably the emissions of pollutants in the atmosphere and slowing down the global warming.

One possible way to convert solar energy into thermal energy is by the use of solar air heaters (SAHs), which consists of a channel, whereby the working fluid (in the case, air) will flow, an insulated plate at the bottom, an absorber plate, heated by the solar energy, at the top and a cover involving it all (Rajarajeswari and Sreekumar

, 2016, and Ansari and Bazargan, 2018). Figure 1 shows a schematic view of a SAH. The air will be heated throughout all the extension of the SAH and it will leave the channel with a higher temperature for several uses, such as ambient heating and fruits and grains drying. Nevertheless, as pointed out by Yadav and Bhagoria (2013), one of the drawbacks of the SAHs is the low thermal efficiency, which depends greatly in the convective heat transfer coefficient.

In order to increase the heat transfer between the absorber plate and the flowing air, longitudinal vortex generators (LVGs) are installed on the absorber plate. As remarked by Song et al. (2016), the longitudinal vortices significantly improve the heat transfer in steady flow and they present a small pressure loss besides potentially enhancing the heat transfer, being more efficient than the transverse vortices.

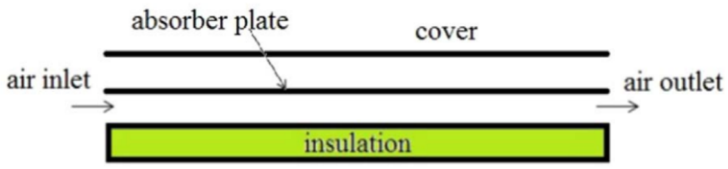

Figure 1. Typical solar air heater. (Kabeel et al., 2017).

2. METHODOLOGY

The geometry of the domain and the flow conditions will establish the parameters used to calculate the pressure loss and the heat transfer. The Reynolds number (Re_{Dh}) will define the fluid flow regime for the internal flow, and the Nusselt number (Nu) and friction factor (f) are used to calculate the thermo-hydraulic performance. The above mentioned dimensionless parameters are determined as

$$Re_{\mathrm{Dh}} = \frac{\rho u_{in} D_h}{\mu} \tag{1}$$

$$Nu = \frac{hD_h}{k} \tag{2}$$

$$f = \frac{2\Delta P D_h}{\rho {u_{in}}^2 L} \tag{3}$$

in which u_{in} is the averaged velocity in the channel entrance, D_h is the hydraulic diameter in the channel entrance, μ is the air dynamic viscosity, ρ is the air density, k is the air thermal conductivity, $\Delta P = P_{in} - P_{out}$ (P_{in} is the averaged air pressure at the domain inlet and P_{out} is the averaged pressure at the domain outlet) and L is the channel length.

As shown in Fig. 2, the geometric parameters of the LVGs are independent for each row, meaning it is possible to assign different values of chord, height and angle of attack for each pair separately. The values of chord (c), height (h) and angle of attack (θ) vary between the following intervals: 8 mm ≤ c ≤ 40 mm, 8 mm ≤ h ≤ 21 mm and 15° ≤ θ ≤ 45°.

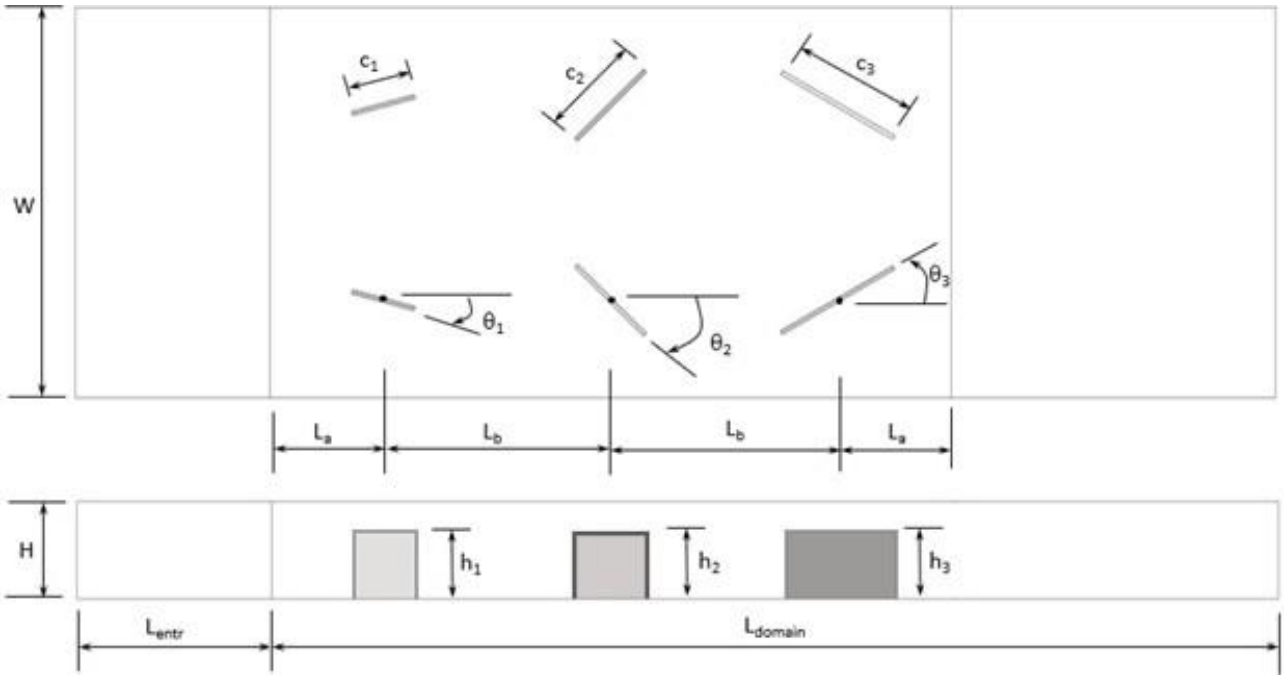

Figure 2. Computational domain and main dimensions.

The rectangular channel, of dimensions 370 mm × 120 mm × 30 mm (L × W × H), is divided into two regions: entrance region, which is responsible for stabilizing the flow before it gets to the second region, the core domain, which contains the LVGs. From Fig. 2, it can be observed that the entrance region has a length of L_{entr} = 60 mm and the core domain has a length of L_{domain} = 310 mm, while the fixed nodes are located in the distances L_a = 30 mm and L_b = 75 mm and from these points the LVGs are constructed and rotated. The LVGs thickness is considered constant, assuming the value of 1.20 mm.

The upper wall is considered adiabatic (q" = 0) and the lower wall, it means, the absorber plate, along with the RWLs, are subjected to a constant heat flux of 1,000 W/m². At the inlet domain, it is imposed a constant velocity of 0.31474 m/s considering the Reynolds number of 1,000, while at the outlet domain, it is imposed a constant pressure of 0. Periodic condition is set for both sides of the computational domain. Moreover, the non-slip condition is considered for all the walls and RWLs.

The governing equations are solved by the software ANSYS® Fluent 19.1. Fluent software is based on the Finite Volume Method (FVM), a discretization technique that transforms the partial equations representing conservation laws over differential volumes into discrete algebraic equations over finite volumes.

According to Saltelli et al. (2019), the Sensitivity Analysis (SA) gives information on the importance of the input variables of a model and their influence on the response of this model. Put differently, it will be analyzed the influence that each input variable has on the output of the studied model and the interactions the input variables present among themselves affecting the output. According to Li et al. (2018), the Latin Hypercube Sampling (LHS) is a regression method that will make a limited number of runs, varying the values of the input variables respecting their intervals and the increments given, with the objective of covering all the design space.

In order to analyze the data coming from the LHS runs and provide the information of the input variables influence on the output, it will be used the Smoothing spline analysis of variance (SS-ANOVA), a non-parametric statistical metamodeling algorithm based on a function decomposition able to extract information from noisy data, identifying relationships among the provided data through modeling them and interpreting them along with the predicted outcome; the SS-ANOVA is able to identify the main effects, it means, the effects of the input variables on the output variables, and the interaction effects, that is, the effects the input variables present interacting between themselves, and they are given in the form of a percentage of each of the contribution to the global variance.

3. NUMERICAL VALIDATION

Three mesh refinements (coarse, intermediate and fine) have been chosen, following the criteria required by the GCI (Grid Convergence Index) method, for the grid independence analysis. As suggested by Celik et al. (2008), the GCI method requires a refinement factor greater than 1.3. Consequently, the three meshes were elaborated in order to agree with the mesh refinement factor minimum criterion. For the mesh independence analysis, it was selected an RWL configuration which generated intense longitudinal vortices. The parameters used were $c_1 = c_2 = c_3 = 40$ mm, $h_1 = h_2 = h_3 = 21$ mm and $\theta_1 = \theta_2 = \theta_3 = 45°$. Table 1 shows the results for friction factor and averaged Nusselt number.

For the numerical validation, the results for Nusselt number and friction factor foreseen by the numerical model for a flat channel with a height-to-width ratio of 1:2 and constant heat flux in all the walls were compared with the results available in Incropera et al. (2007). The results are shown in Fig. 3. It can be seen the relative errors are, respectively, 3.64 % and 3.39 %, validating the numerical procedure.

Table 1. GCI values for the fine mesh.

		Fine Mesh	Intermediate Mesh	Coarse Mesh
Volumes number, n		9,946,802	3,745,493	1,652,995
Mesh refinement factor, r		-	1.3848	1.3134
CPU time		181 minutes	62 minutes	26 minutes
GCI	f		0.241 %	
	$\overline{Nu}$		0.072 %	

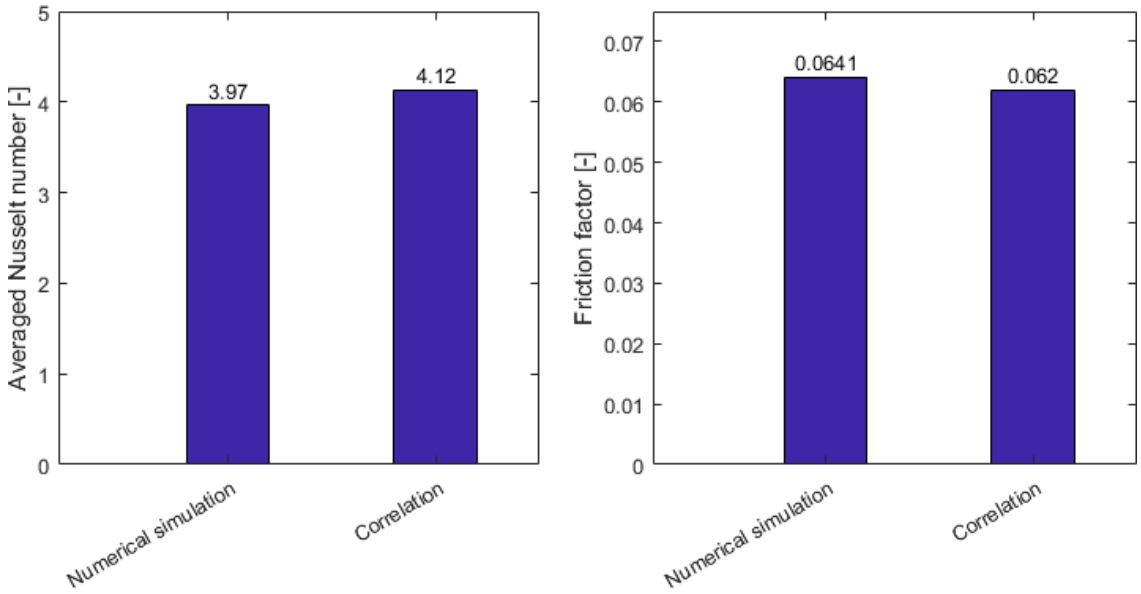

Figure 3. Comparison between the numerical results and correlations.

4. RESULTS AND DISCUSSION

The results of SS-ANOVA are presented in Fig. 4 to Fig. 7. Figure 4 and Fig. 5 represent Nusselt and friction factor respectively for RWL in common-flow-up and Fig. 6 and Fig. 7 the respective counterparts for common-flow-down configuration.

Comparing Fig. 5 and Fig. 7, which show the contribution of each parameter on the friction factor for RWLs in the common-flow-up and common-flow-down configurations, respectively, overall, the parameters present almost the same behavior contributing on friction factor, only with small differences on the order of the main parameters, while for the parameters contributing on the Nusselt number for RWLs in the common-flow-up and common-flow-down configurations, as shown in Fig. 4 and Fig. 6, respectively, all main effects present for the common-flow-down configuration also show up for the common-flow-up configuration, however, the common-flow-down configuration presents a high number of interaction effects. Some of the conclusions are exposed below.

It can be observed from Fig. 4 to Fig. 7 the input parameter which most contributes on the thermo-hydraulic parameters is c_1 (except for the friction factor in common-flow-down configuration, which presents h_3 as the first one and c_1 as the second one, but with very close contributions). In general, c_1 and h_3 present approximately the same contribution on the friction factor for both configurations, as can be seen in the sensitivity analysis, as shown in Fig. 5 and Fig. 7, while h_3 has negligible contribution on the Nusselt number — Fig. 4 and Fig. 6 — meaning it is possible to set a high value for c_1 and, in order to counteract the increase of the friction factor, set a low value for h_3.

As already said, Fig. 4 and Fig. 6 show h_3 presents a negligible contribution on the Nusselt number, whereas, observing Fig. 5 and Fig. 7, the contribution on the friction factor reaches a sufficient value no to be unconsidered. Observing the sensitivity analysis, it is possible to realize h_3 is the first and the second variable which most influences the friction factor for common-flow-down and common-flow-up configurations, respectively, in Fig. 7 and Fig. 5, with a contribution of 11.7 % and 11.5 %, but a contribution of only 0.1 % on the Nusselt number for both configurations (Fig. 4 and Fig. 6). This variable needs to be as low as possible, not only in order to counteract the increase of the friction factor due to the high value of c_1, but also because, broadly speaking, it only causes the augmentation of the friction factor.

The angles of attack themselves of the three rows of LVGs contribute approximately the same to the Nusselt number and to the friction factor in the common-flow-up configuration, respectively, as Fig. 4 and Fig. 5 show. On the other hand, the sensitivity analysis shows that, for both output variables, θ_1 has the approximate same interaction effect with c_1, which, in its turn, influences much more the Nusselt number than the friction factor. It leads to the conclusion it is advantageous to set a high value for θ_1 with the objective of influencing positively c_1 and, consequently, the Nusselt number. When analyzing θ_3, for the Nusselt number, it presents almost no interaction with other parameters, however, for the friction factor, it has some influence on h_3 and c_3, which are, respectively, the second and the third parameters which most influence the friction factor, presenting almost the same contribution as the first one. It leads to the conclusion it is better to set low values for θ_3.

As can be observed in Fig. 6, for the common-flow-down configuration, the only angle of attack which presents a main effect on the Nusselt number is θ_1, while the other ones present a negligible main effect contribution; however, it is observable a high degree of interaction between the parameters, mainly with regard to θ_2, interacting, among other parameters, with c_1 and θ_1, the first and third parameters, respectively, which most contribute to the friction factor, as seen in Fig. 7. Otherwise, the angles of attack of all the three rows of LVGs present significant main effect on the friction factor. It leads to the conclusion that θ_3 should be small, while θ_2 should be set high in order to influence positively c_1 and θ_1 and, consequently, the Nusselt number; moreover, θ_2 is the angle of attack with the least contribution on the friction factor and the least contributing parameter of the main ones.

Observing Fig. 5 and Fig. 7, which present the contribution of the parameters on the friction factor for both configurations, it is observable almost main effect is shown up, while only two interaction effects are present; the only main effect that does not appear in the list of the first ten most contributing parameters is h_2, evidencing a low degree of interaction effects between the inputs influencing the friction factor.

A similar analysis can be made for the inputs contributing on the Nusselt number: Fig. 4 shows in the common-flow-up configuration, seven out of the nine main effects are shown up, while the other three most contributing parameters are interaction effects; once more, h_2 is not among the main parameters. Again, there is a low degree of interaction effects between the inputs influencing the Nusselt number. Now analyzing the common-flow-down configuration, Fig. 6 shows only four out of the ten main parameters are main effects, whilst the other six are interaction effects, evidencing a high degree of interaction. Three variables deserve to be highlighted: h_3 is not among the main parameters as main effect neither as an interaction effect; c_3, although being one of the first ten most contributing parameters, occupies the last position, presenting a little contribution on the Nusselt number of only 1.9 %; θ_3, in spite of appearing in the main parameters list as an interaction effect, interacts with c_3, which is, as already said, the last one among the main parameters; these three variables above mentioned, besides contributing only a little to the Nusselt number, present a significant influence on the friction factor, as seen in Fig. 7, meaning they need to assume low values. It is observable all the parameters related with the third row of RWLs should be set with small values, or in other words,

the third row causes an augmentation of the friction factor with a little contribution on the Nusselt number, mainly because there is only a little area left of heated plate behind it for the heat exchange to happen.

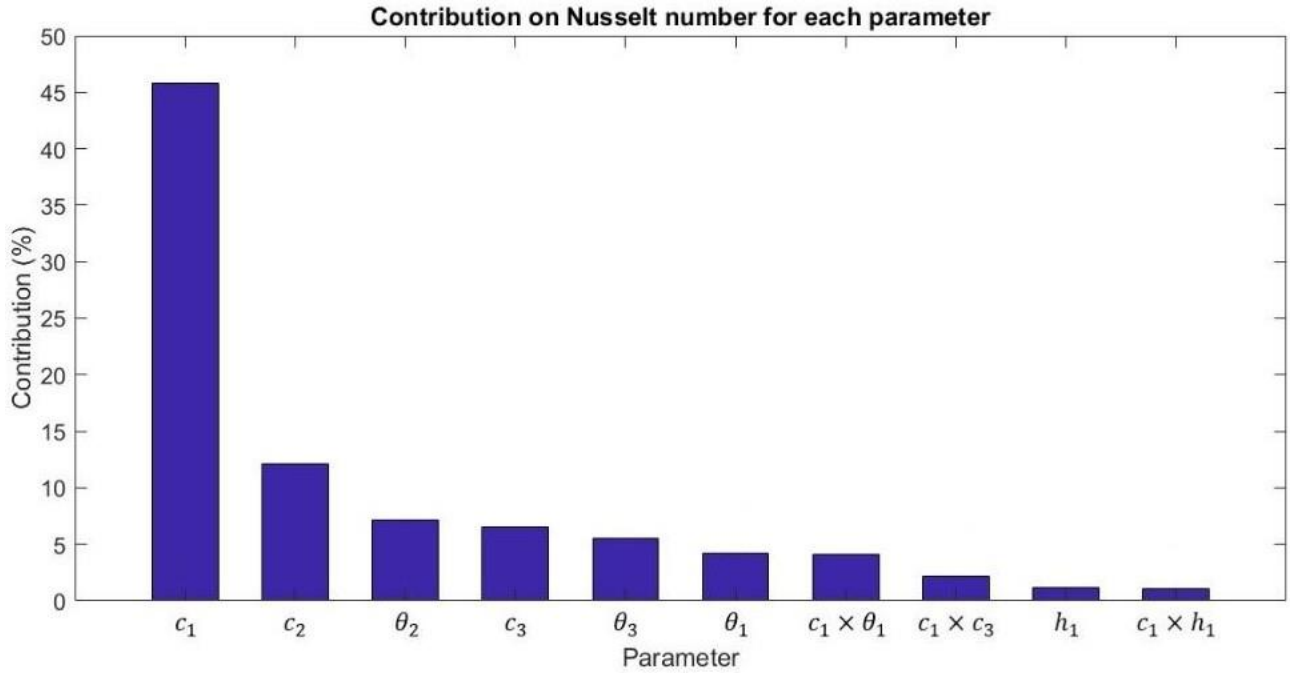

Figure 4. Contribution of the main parameters on the Nusselt number for the RWLs in common-flow-up configuration.

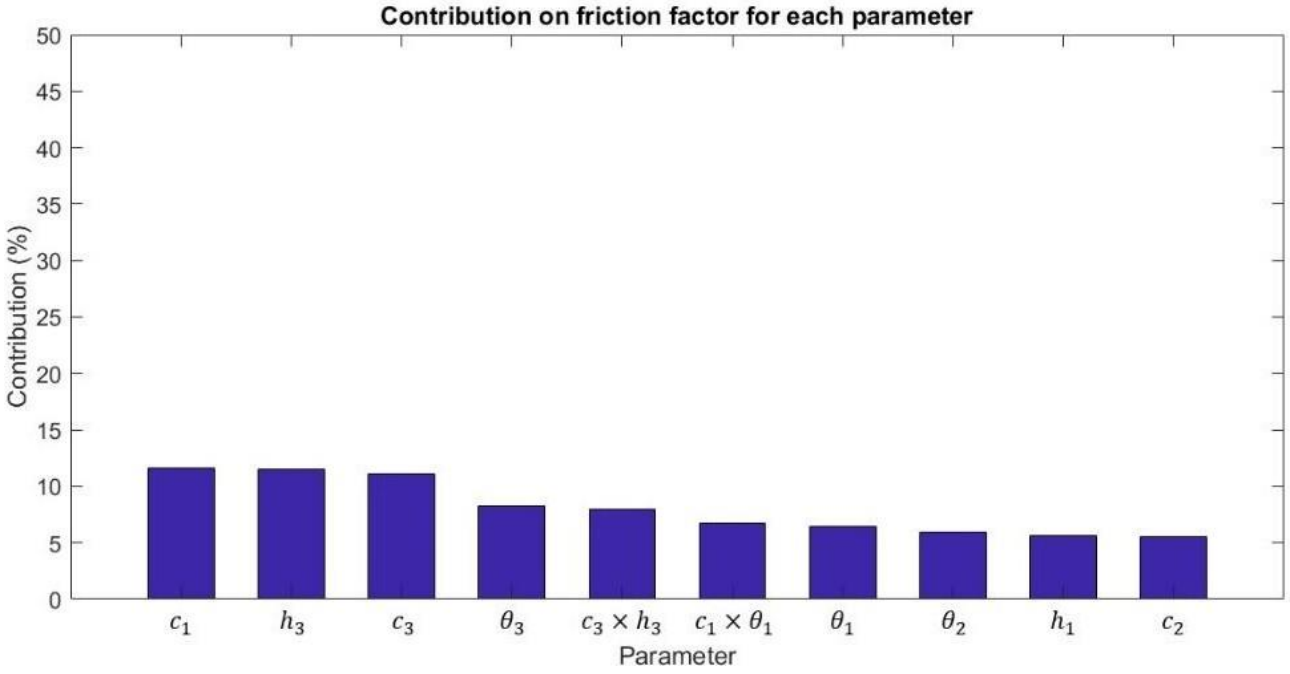

Figure 5. Contribution of the main parameters on the friction factor for the RWLs in common-flow-up configuration.

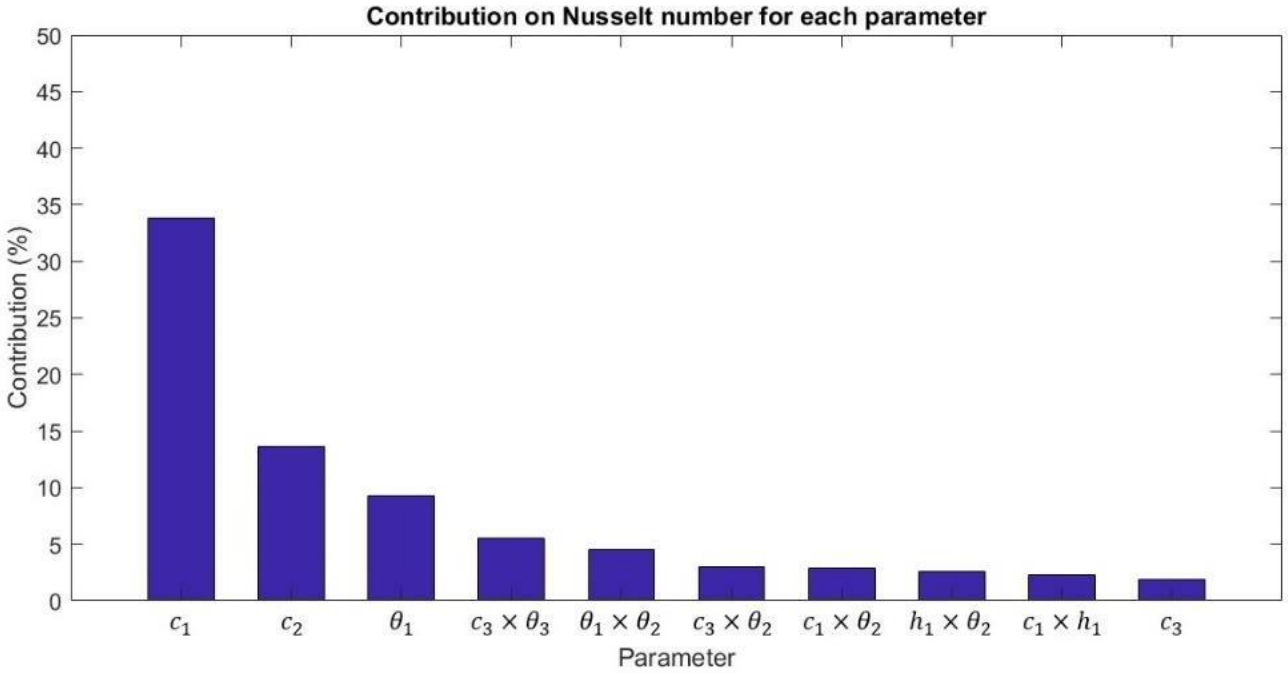

Figure 6. Contribution of the main parameters on the Nusselt number for the RWLs in common-flow-down configuration.

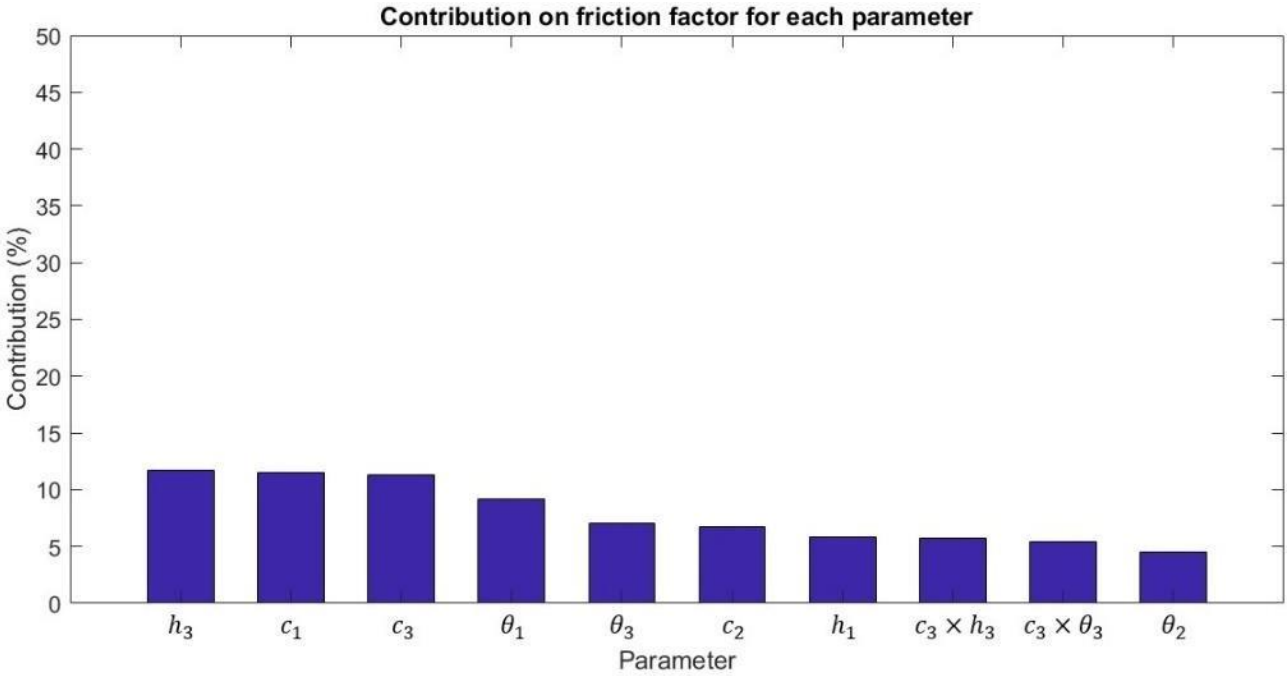

Figure 7. Contribution of the main parameters on the friction factor for the RWLs in common-flow-down configuration.

5. CONCLUSIONS

The present research studied the heat transfer enhancement and associated pressure loss of a laminar flow, with a Reynolds number of 1,000, in a rectangular entrance channel with RWLs, and the method used to analyze the obtained results was the SS-ANOVA.

The SS-ANOVA method is capable of providing the results of main effects and interaction effects, with the following principal results: the RWLs in both configurations present similar behaviour on the friction factor with few interaction effects, but different behaviour on the Nusselt number, with a high number of interactions for the common-

flow-down configuration. All the parameters related with the third row of RWLs in the common-flow-down configuration should be small in absolute values, while θ_2 should be high. θ_3 should also be small for the common-flow-up and h_3 should be small for both configurations. For the common-flow-up configuration, it is possible to observe a small frontal area of the first and last rows of RWLs, while for the common-flow-down, small angles of attack are noticeable.

6. ACKNOWLEDGEMENTS

The authors would like to acknowledge São Paulo Research Foundation (FAPESP), grant numbers 2017/06978-3 and 2018/04639-0, for the financial and technical support.

7. REFERENCES

Ansari, M. and Bazargan, M., 2018. "Optimization of flat plate solar air heaters with ribbed surfaces". *Applied Thermal Engineering*, Vol. 136, pp. 356–363.

Celik, I.B., Ghia, U., Roache, P.J., Freitas, C.J., Coleman, H. and Raad, P.E., 2008. "Procedure for Estimation and Reporting of Uncertainty Due to Discretization in CFD Applications". *Journal of Fluids Engineering*, Vol. 130, pp. 078001-1–078001-4.

Incropera, F.P., DeWitt, D.P., Bergman, T.L. and Lavine, A.S., 2007. *Fundamentals of Heat and Mass Transfer*. John Wiley & Sons, Inc., 6th edition.

Kabeel, A.E., Hamed, M.H., Omara, Z.M. and Kandeal, A.W., 2017. "Solar air heaters: Design configurations, improvement methods and applications – A detailed review". *Renewable and Sustainable Energy Reviews*, Vol. 70, pp. 1189–1206.

Li, H., Wang, S. and Cheung, H., 2018. "Sensitivity analysis of design parameters and optimal design for zero/low energy buildings in subtropical regions". *Applied Energy*, Vol. 228, pp. 1280–1291.

Rajarajeswari, K. and Sreekumar, A., 2016. "Matrix solar air heaters – A review". *Renewable and Sustainable Energy Reviews*, Vol. 57, pp. 704–712.

Saltelli, A., Aleksankina, K., Becker, W., Fennell, P., Ferretti, F., Holst, N., Li, S. and Wu, Q., 2019. "Why so many published sensitivity analyses are false: A systematic review of sensitivity analysis practices". *Environmental Modelling & Software*, Vol. 114, pp. 29–39.

Schutz, F., Massuquetti, A. and Alves, T.W., 2013. "Demanda e oferta energética: uma perspectiva mundial e nacional para o etanol". *Revista Eletrônica em Gestão, Educação e Tecnologia Ambiental – REGET*, Vol. 16, pp. 3167–3186.

Shahsavari, A. and Akbari, M., 2018. "Potential of solar energy in developing countries for reducing energy-related emissions". *Renewable and Sustainable Energy Reviews*, Vol. 90, pp. 275–291.

Song, K., Liu, S. and Wang, L., 2016. "Interaction of counter rotating longitudinal vortices and the effect on fluid flow and heat transfer". *International Journal of Heat and Mass Transfer*, Vol. 93, pp. 349–360.

Yadav, A.S. and Bhagoria, J.L., 2013. "Heat transfer and fluid flow analysis of solar air heater: A review of CFD approach". *Renewable and Sustainable Energy Reviews*, Vol. 23, pp. 60–79.

8. RESPONSIBILITY NOTICE

The authors are the only responsible for the printed material included in this paper.